Compression-Molded Three Dimensional Tapered Optical Polymeric Waveguides for Optoelectronic Packaging

Suning Tang
Radiant Research, Inc.
3925 W. Braker Lane, Suite 420
Austin, Texas 78759
Phone: 512-305-0297

Linghui Wu, Felming Li, Ting Li, and Ray T. Chen
Microelectronics Research Center
Department of Electrical and Computer Engineering
University of Texas, Austin, Texas 78712-1084
Phone: 512-471-7035

ABSTRACT

It is one of the major bottlenecks to bridge various optoelectronic devices, such as laser diodes, optical waveguides and photodetectors in ultra low-loss optoelectronic interconnects, which are often fabricated using different technologies with different optical apertures. To solve this problem, three dimensional (3D) tapered optical polymeric waveguides are presented to provide the mode-matching among these optoelectronic components. Compression-molded polymeric waveguides presented herein is probably the only solution to bridge huge dynamic range of different optoelectronic device-depths varying from few microns to few hundreds microns. Both the design rule and fabrication technique are presented together with some experimental results. It is shown that such a 3D tapered waveguide can provide an effective optical coupling at a relaxed alignment tolerance.

1. INTRODUCTION

By now, many of the key components required to realize the optical communication networks have reached an appreciable state of maturity. On the one hand, impressive performance data have been obtained for a large variety of optoelectronic active devices including lasers, amplifiers, electro-optic switches, modulators, and detectors. On the other hand, the transmission characteristics achieved for the optical waveguides and fibers are very close to allow optical transmission spans in any dimension of interest, from intra-wafer interconnection to global optical communication. However, the full exploitation of these marvelous achievements is hindered by the bottleneck that appears at the interfaces among all these components that are often fabricated in different substrates with different dimensions. For example, laser diodes can be made in GaAs, detectors in silicon, and modulators in $LiNbO_3$. The dimension of each type of device is often pre-chosen to optimize its own performance. It has been realized that it is difficult to achieve efficient optical couplings among these devices with a large alignment tolerance by using prism, grating, or optical lens. The problem is that the dynamic range of these optoelectronic components varies from few microns (single-mode waveguides and vertical cavity surface-emitting lasers) to hundreds of microns (photodetectors and multimode fibers). Three problems occurs at the interfaces: (1) the inconveniently high coupling loss due to the optical mode mismatch, (2) the strict alignment tolerance, and (3) pixel separation mismatch when the laser diode array, smart pixel array, photodetector array and optical fiber/waveguide array are employed. Due to the planarized nature of these devices mentioned above, the most common approach based on microlens is too expensive because it requires the complicated three spatial and three angular multiple alignments. An effective method is needed to effectively couple light from one device to another at a relaxed alignment tolerance.

Two dimensional tapered waveguides have been proposed and employed to improve the optical coupling among various optoelectronic devices[1-6]. However, there is no existing optoelectronic/microelectronic fabrication method that is able to provide the required three-dimensional (3D) dynamic range, varying from few microns to hundreds of microns. In this paper, the compression-molding technique[7] is investigated to fabricate the 3D tapered polymer-based waveguide couplers for

SPIE Vol. 3005 • 0277-786X/97/$10.00

cost-effective, low-loss coupling among optoelectronic components. The idea is to take the advantage of plastic characteristics of optical polymer and create a compression-molded 3D horn-shaped waveguide (array) to provide adiabatic optical transition regions between the optoelectronic devices that have different mode profiles and different pixel separation. As a result, both the coupling efficiency and the alignment tolerance can be significantly improved at a reduced fabrication cost. For example, Fig. 1 shows an application of the 3D tapered waveguides, where the optical signals from a VCSEL array can be effectively coupled into a multimode optic fiber array. The compression-molded polymeric waveguides employed herein may be the only solution to bridge the huge dynamic range of different optoelectronic device-depths varying from few microns to few hundreds microns.

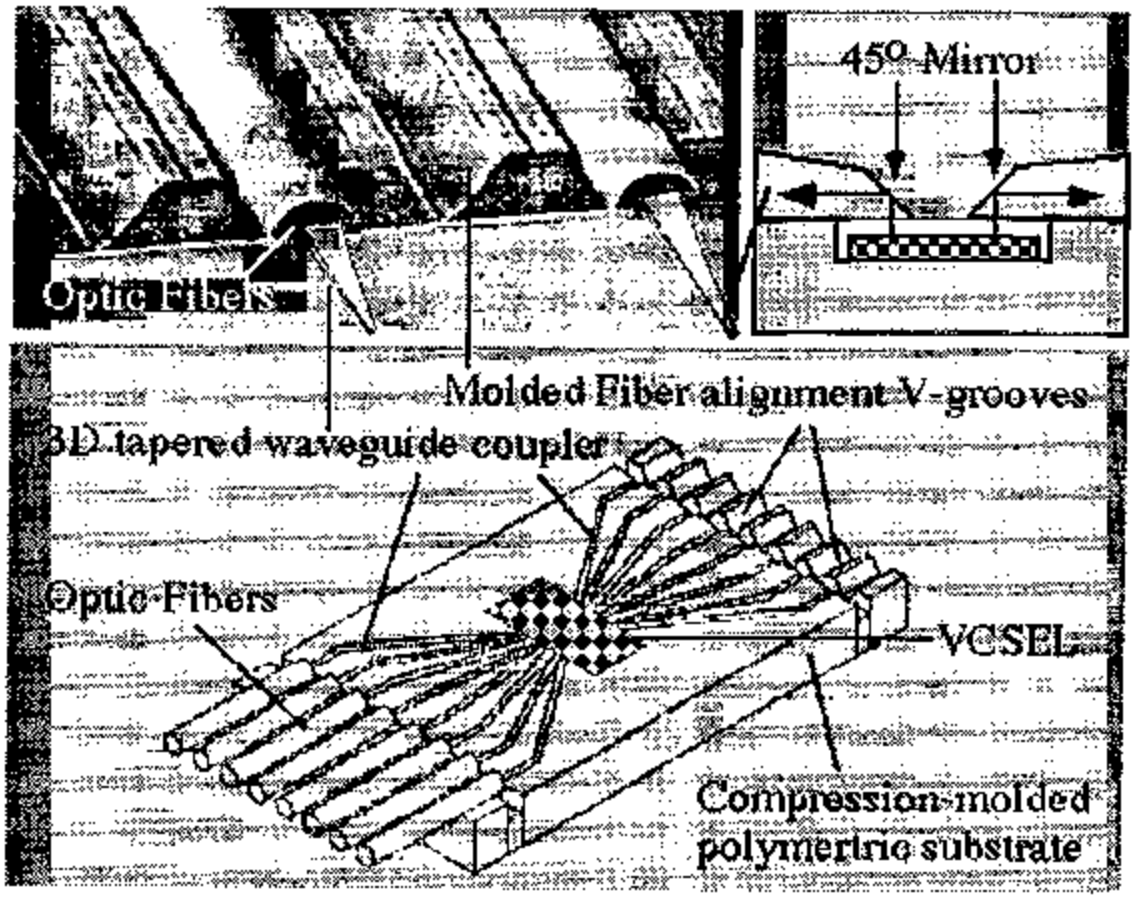

Fig. 1. Compression-molded optical coupling module based on an array of 3D tapered waveguide couplers, VCSELs, where the optical signals from the VCSEL array can be effectively coupled into a optic fiber array.

2. DERIVATION OF THE CRITICAL SLOPE OF A 3D TAPERED WAVEGUIDE COUPLER

Fig. 2 illustrate the top and side view revealing the basic structure of the 3D tapered polymer-based coupling device that can be employed, for example, to improve the optical coupling between a single-mode waveguide laser to a multimode fiber/waveguide. In order to provide a low loss transition, the tapered waveguide must operate adiabatically, in other wards, the lowest order local normal mode of the structure must propagate through the structure without cumulative power transfer to higher order local normal modes. There have been a number of instructive computer investigations of mode conversion in tapered waveguide horns[8-11], trying to develop a general design rule that would be applicable to all horns and at all operation wavelength.

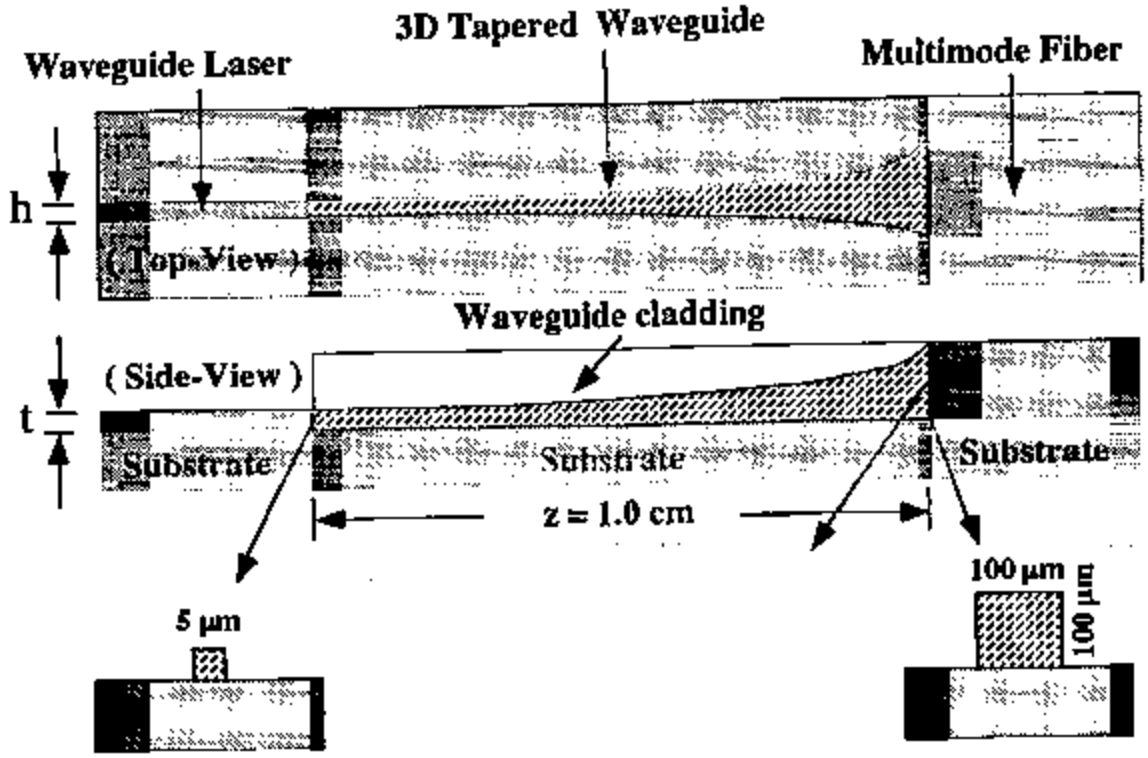

Fig. 2. Schematic of the integrated tapered waveguide that can be used to improve the optical coupling efficient between a small waveguide device and a large waveguide device.

In our analysis, a simplified approach based on the scalar wave equation is employed. We assume that the tapered waveguide can be subdivided into many small waveguide sections labeled by an index ν, where each segment is defined by a refractive index distribution $n^{\nu}(x,y)$ independent of z. With the notation $\Phi_m^{\nu}(x,y)$ and β_m^{ν} for the local normal modes of order m and their associated propagation constants, respectively, the scalar wave equation for segment ν reads,

$$[\frac{\partial^2}{\partial x^2} + \frac{\partial^2}{\partial y^2} + k^2 n^{\nu 2}(x,y)]\,\Phi_m^{\nu}(x,y) = (\beta_m^{\nu})^2 \Phi_m^{\nu}(x,y) \quad . \qquad (1)$$

Here $k = 2\pi/\lambda$ denotes the wave number corresponding to the free space wavelength λ. In order to calculate the evolution of the field along the tapered waveguide, we note that due to the completeness of the modes, the electric field distribution within each segment can be expressed as

$$E^{\nu}(x,y,z) = \sum a_m^{\nu}(z)\, \Phi_m^{\nu}(x,y) \quad . \qquad (2)$$

Based on the modes calculated from Eq. (1), the field propagating along the structure can be described entirely in terms of the complex amplitudes $a_m^{\nu}(z)$, which can be solved by an iteration of two steps using Fourier analytic approach[12]. First, as long as both z and z+d lie within the same segment ν, propagation is described by

$$a_m^{\nu}(z+d) = a_m^{\nu}(z) \exp(i\beta_m^{\nu} d). \qquad (3)$$

Second, the requirement that the electric field be continuous at the interface $z^{v,v+1}$, between two consecutive segments v and v+1 leads to a simple relationship between the complex amplitudes $a_j^{v+1}(z^{v,v+1})$ and $a_m^{v}(z^{v,v+1})$, i.e.,

$$a_j^{v+1}(z^{v,v+1}) = \sum_{\text{all } m} \langle \Phi_j^{v+1} / \Phi_m^{v} \rangle a_m^{v}(z^{v,v+1}) \quad . \tag{4}$$

Hence, by using Eq. (3) and (4) with the modes $\Phi_m^v(x,y)$ and propagation constants β_m^v obtained from Eq. (1), we may simulate the propagation of the optical field along the tapered waveguide sections.

The 3D tapered waveguide device is designed as an adiabatic device in which the optical power is predominantly guided by the fundamental mode. By keeping track of the excitation spectrum defined by the $\{a_m^v(z)\}$, we can determine where deviations from adiabatic behavior occur. It has been found that the critical taper slope for adiabatic operation can be given as

$$\left(\frac{\partial x}{\partial z}\right)_c = (\beta_0 - kn_{clad}) / \left(\left\langle \frac{\partial \Phi_0}{\partial z} \right\rangle^2\right)^{1/2} \quad , \tag{5}$$

which has to be simulated numerically. For a tapered waveguide with near-square input and output cross sections, Fig. 3 shows the optimized taper profiles that allow an adiabatic transition of a lowest order guided mode propagating along the waveguide taper. The tapered waveguide has a dimension of 5 μm at the small end with single-mode operation.

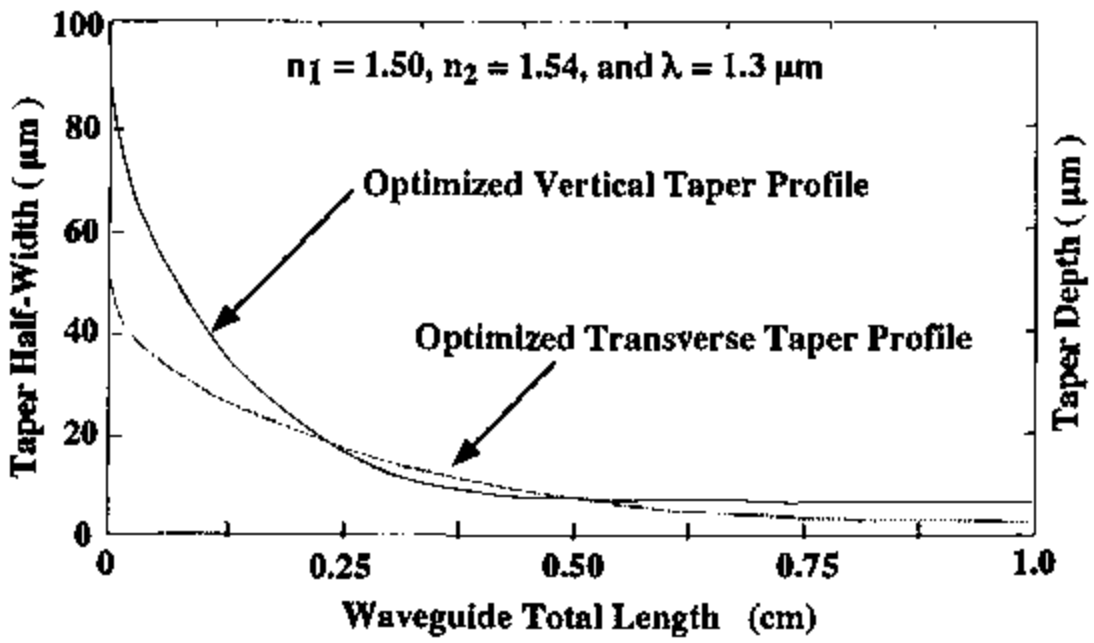

Fig. 3. Optimized taper profiles for adiabatic transition in a 3D tapered channel waveguide.

In practice, a simple design rule, given by

$$\left(\frac{\partial x}{\partial z}\right)_c < 2\tan\left(\frac{\pi}{r\beta_0}\right) \quad , \tag{6}$$

may be followed to ensure adiabatic operation in a tapered waveguide where the lowest order mode is well confined to the guide in the transverse direction[6].

Based on coupled-mode theory, the radiation loss for a tapered waveguide is given by[9]

$$P_{rloss} = (\frac{3n_e}{\pi\lambda})^2 (\frac{d^2 d_0^2}{z})^2 \qquad (7)$$

where P_{rloss} is the power loss normalized by the input power, and d is the waveguide diameter. n_e is the effective index of the tapered waveguide. It should be noted that there is a tradeoff between taper length and taper slope for low loss operation. Small slope is preferred for smooth adiabatic transition (low radiation loss) while short coupler length (large slope) is always desired to reduce the device propagation loss. Fig. 4 shows the radiation losses as a function of the tapered waveguide length based on Eq. (7). For example, for d_{max} = 100 μm and d_{min} = 5 μm, the radiation loss is 3% if n_e = 1.5 and z = 1.0 cm are assumed.

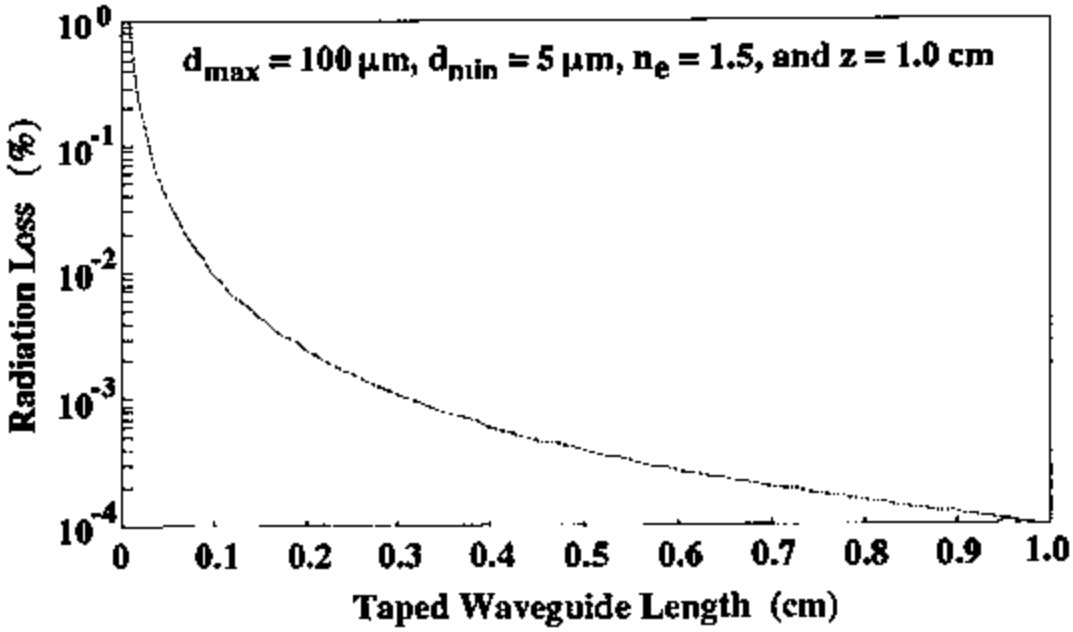

Fig. 4. Radiation loss verses the taped waveguide length calculated based on Eq. (7).

3. FABRICATION OF POLYMER-BASED 3D TAPERED WAVEGUIDE COUPLERS USING COMPRESSION-MOLDING TECHNIQUE

To improve the optical coupling among various optoelectronic guided wave devices, it is highly desired to have the mode profile matching at the coupling interface. This requires that the waveguide dimensions are closely matched at the interface not only horizontally but also vertically. However, there is no existing optoelectronic device fabrication method that is able to provide the required dynamic range three-dimensionally, ranging from few microns to hundreds of microns. In order to overcome this problem, we have developed a compression-molding technique[7] that can be used to fabricate three-dimensional (3D) tapered polymeric waveguides couplers to provide a cost-effective, low-loss coupling solution for optoelectronic components. Based on this technique, we are able to create the desired 3D horn-shaped polymeric waveguide that has different waveguide dimension at the two ends. With proper design, such 3D tapered waveguides can provide adiabatic optical transition between different optoelectronic devices that have different mode profiles. As a result, both the coupling efficiency will be significantly improved. The compression-molded polymeric waveguides employed herein may be the only

solution to bridge the huge dynamic range of different optoelectronic device-depths varying from few microns to few hundreds microns.

3.1 Fabrication of 3D tapered waveguide mold plunger

Precision diamond turning machine (Pneumo Ultra 2000) was employed to fabricate the required mold plunger in order to form the polymer-based 3D tapered waveguide using compression-molding technique. With various gem quality diamond tools, precision microstructure can be generated with one millionth of an inch resolution and surface finishes in nanometers. Fig. 5 shows the main fabrication steps for the realization of a 3D tapered mold plunger. Naval brass was selected as the master substrate, which yields good results in diamond turning due to its homogeneity. It also works very well for the electroplating process of the master die. The brass substrate was first mechanically polished. After metrological testing, an array of 3D tapered waveguide structure (female) was created by using a precision diamond turning machine. The finished master die was then bought to electroforming process that includes the following steps, preplanning, masking, final cleaning, passivation, electroplating, and separation. Nickel electroforming was selected based on its hardness and chemical stability. This process can produce fine surface detail with great accuracy. The mechanical and physical properties of the electroforming can be closely controlled by the solution and the conditions of deposition. Bright, and smooth surfaces can be generated without the need for polishing or machining individual components after fabrication. Fig. 6 is the photo picture of the 3D mold plunger fabricated. Note that a linear tapered was employed for simplicity.

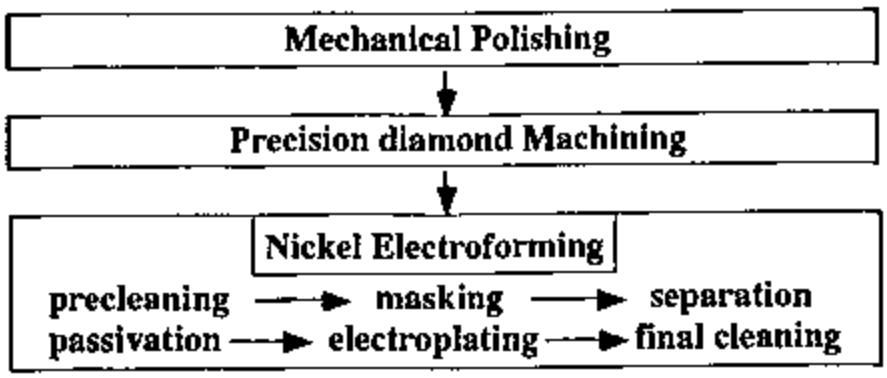

Fig. 5. Schematic diagram of fabrication of 3D tapered waveguide mold plunger using precision diamond machine.

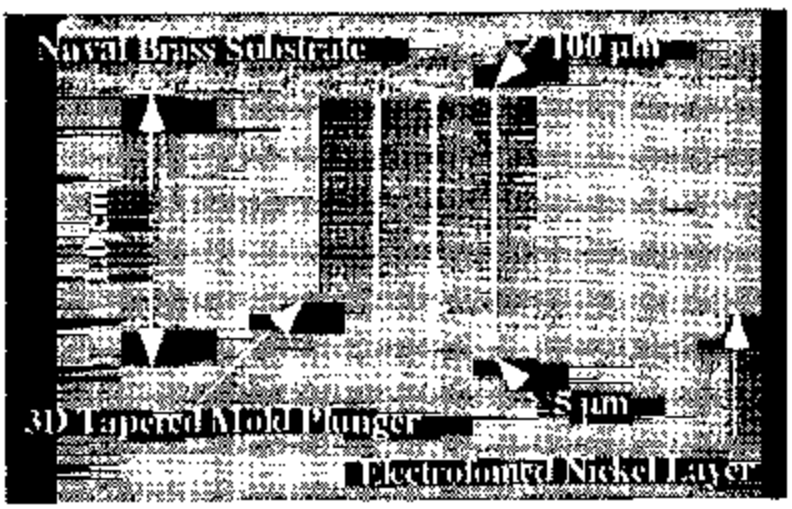

Fig. 6. Photograph of the 3D linear tapered waveguide mold plunger fabricated.

3.2 Fabrication of Compression-Molded 3D Tapered Waveguide Coupler

The process of compression molding is described by reference to Fig. 7. A two-piece mold provides a cavity having the shape of the desired 3D tapered waveguide. An appropriate amount of molding material, polymer waveguide film in this case, is spin-coated or laminated onto the substrate of interest. The film thickness is equal to the maximum thickness of the tapered structure. Due to the nature of compression molding, the shape of the molded waveguide is completely defined by the shape of the mold plunger. The molding process begins with heating of the mold plunger and the polymer film. Then the compression molding is carried out by bringing the two parts of the mold together under pressure. The polymer film, softened by heat, is thereby welded into the shape of the stamp. The last step is to harden and fix the molded waveguide shape. If the polymer is thermosetting, the hardening is effected by further heating under pressure in the mold. If it is a thermoplastic, the hardening is effected by chilling. For some special photo polymers, this process can be fulfilled by UV exposure. These fundamental differences in polymers dictate the plastic processing method to be used in the waveguide molding[16-20]. After polymer is cured (fixed), the mold plunger can be removed, and the 3D tapered waveguides are formed.

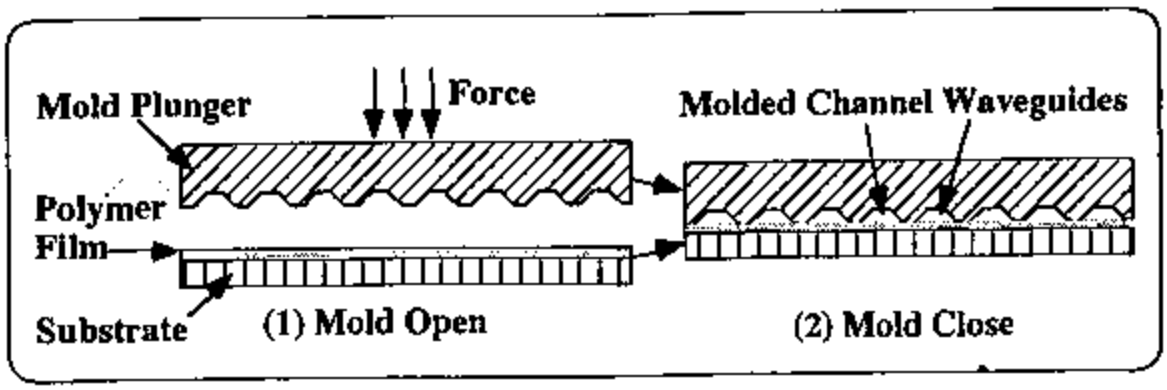

Fig. 7. Schematic of the two-piece of compression molding technique to form 3D tapered waveguide.

A compression-molded 3D tapered waveguides have been fabricated using photolime gel[5]. Fig. 8 shows the 3D tapered waveguides fabricated by the compression-molding technique. The molding tool that we employed has a waveguide width (t) and height (h) of 5 μm at the small end. It is 3D linearly tapered with a waveguide width and height of 100 μm at the large end. A small section of the molded polymer waveguide is shown in Fig. 9 where the 3D tapering is clearly indicated. The waveguide thus fabricated demonstrated multiple modes without a cover cladding. However, it becomes single-mode operation at the small end if a polymeric cladding layer is further spin-coated on it. It is to be noted that the molding process shall be performed during the phase transition period within which the polymer film is deformable. The thickness of guiding layer is controlled by the pressure between the molding plunger and glass substrate. The exclusive characteristic of the polymer thin film, i.e., photolime gel, employed herein has the graded index (GRIN) distribution which allows us to fabricate these molded waveguide devices on any substrate of interest regardless of the substrate refractive index and conductivity.

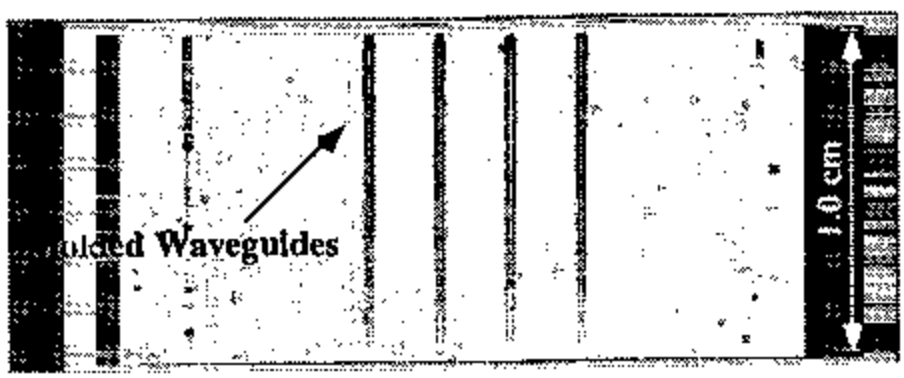

Fig. 8. Photograph of compression-molded 3D tapered waveguides based on photolime gel polymer.

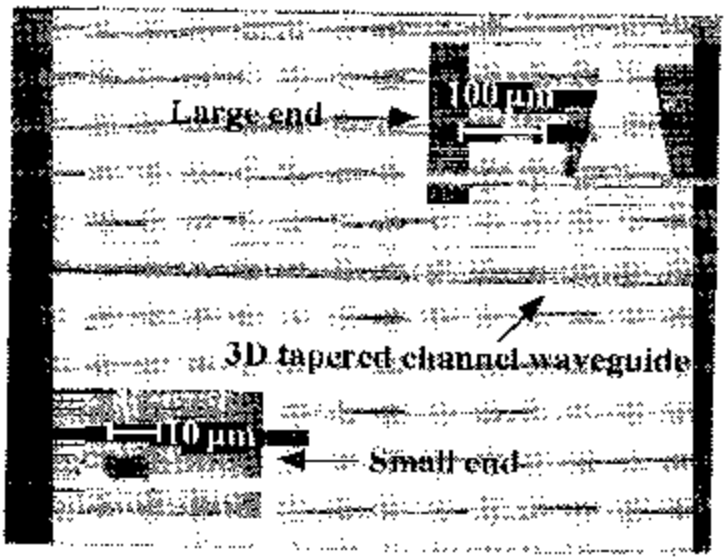

Fig. 9. Photopicure of a small section of the molded 3D linear tapered waveguide fabricated. The cross sections of the two ends are also shown in the figure.

It should be noted that not only the vertical depth variation but also the linear dimension of such molded waveguides are well beyond the limits that any other conventional waveguide fabrication methods. Fig. 10 illustrates a 45 cm long compression-molded channel waveguide made on a glass substrate, where a microprism [21] is employed to coupled 632.8 nm HeNe laser beam into the waveguides. In the experiment, the phase matching angle was set at the E_{11}^{x} mode. Waveguide propagation losses of different samples were measured using the two prism method. Loss figures from 0.5 to 2 dB/cm were experimentally confirmed at 632.8 nm. Previous demonstration using crosslink technique had a measure loss of 0.1 dB/cm at 1.3 μm[12]. Such a polymeric waveguide is the longest achieved thus far. The large linear dimension is well above that can be provided through conventional microlithography and is thus useful for optical interconnect hierarchy requires longer interconnection distance.

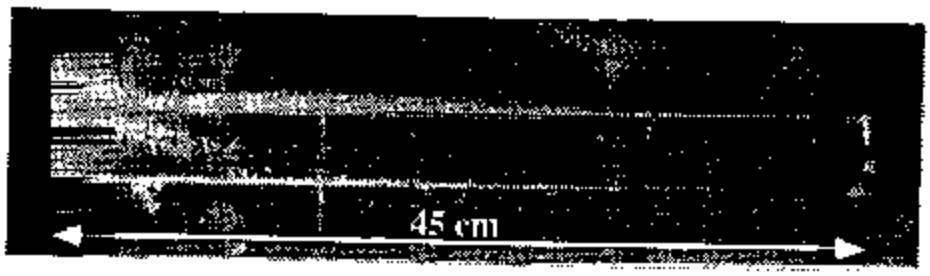

Fig. 10. A 45 cm long compression-molded channel waveguide on a glass substrate using photolime gel polymer.

Unlike most of the optical polymeric materials, which are synthesized in the laboratories, the polymer we employed in this experiment, photolime gel, are extracted from animal tissues. We have demonstrated an array of integrated photonic devices using this polymeric material. These include planar waveguide[21], linear and curved channel waveguide arrays[22], traveling wave electro-optic waveguide modulator[23,24], multiplexed waveguide hologram[25-26], Nd^{+++}-doped waveguide amplifier working at 1.06 μm[27]. Furthermore, the graded index characteristic of the waveguide allows the formation of high quality of waveguide devices on any substrate of interest. Therefore, this integrated photonic device technology can be transfer to any substrates. The polymeric solutions with various photolime gel and water ratios can be easily prepared and then spin-coated on glass substrates.

4. CHARACTERIZATION OF COMPRESSION-MOLDED 3D TAPERED WAVEGUIDES

In order to estimate the loss introduced by the tapered structure, a straight channel waveguide has been fabricated with channel dimensions t = h = 5 μm, which is equal to the tapered waveguide dimensions at the small end. The tapered waveguide has a waveguide length of 1.0 cm and the straight channel waveguides have the channel lengths of 1.0 cm, 2.0 cm, 3.0 cm, and 5.0 cm. Light from a HeNe laser operating at 0.6328 μm was coupled into a single-mode fiber having core diameter of 5 μm. The end of fiber was then butt-coupled to the channel waveguide and tapered waveguide, respectively, with the aid of index matching fluid. The transmission through the waveguide was measured by a Si photodetector. After removing the waveguide under test, the total power merging from the fiber was measured. The waveguide propagation loss and the coupling loss are 0.5 dB/cm and 0.7 dB, respectively. Reflection at the exit end of the waveguide accounts for 0.15 dB of the coupling loss, and hence the loss due to mismatch between the input wave function and that of the waveguide is 0.55 dB. By comparing the transmission loss difference, the radiation loss introduced by the tapered structure is measured and determined about 0.2 dB/cm. This radiation loss depends on the shape of the waveguide as described in Eq. (7).

To demonstrate the coupling improvement by using 3D tapered waveguide coupler, the insertion losses were measured by direct end-butt coupling from a single-mode fiber to a multimode fiber and by end-butt coupling through a 3D tapered waveguide coupler. The core diameter is 5 μm for the single-mode fiber and 100 μm for the multimode fiber. The 3D tapered waveguide has waveguide dimension of 5 μm (t = h) at the small end and of 100 μm at the large end. The length of the 3D tapered waveguide is 1.0 cm. The lowest insertion loss for the direct end-butt coupling in this case is 3 dB while the lowest insertion loss for the coupling using a 3D tapered waveguide coupler is less than 1.2 dB. Hence, the net improvement provided by the taper is 1.8 dB. We conclude that even with the additional loss introduced by the tapered region, the total coupling efficiency can be improved by using the 3D tapered waveguide couplers.

5. CONCLUDING REMARKS

We report the first compression-molded 3D tapered waveguide fabricated by using compression-mold technique. Not only the vertical depth variation but also the linear dimension of the molded waveguides are well beyond the limits that any other conventional waveguide fabrication methods. The molded waveguides with a vertical depth of 95 μm in 1.0 cm length has been demonstrated using a photolime gel polymer. A channel waveguide with a linear dimension of 45 cm is also demonstrated. Among all the thin film waveguides reported, polymer-based optical waveguides have been widely agreed to be the best candidates due to their cost-effectiveness, low dielectric constant for multilayer coating and feasibility of conducting 3D optical interconnects. Compression-molded polymeric waveguides presented herein is probably the only solution to bridge huge dynamic range of different optoelectronic device-depths varying from few microns to few hundreds microns. The concept presented herein can be used to mold any polymer-based thin film with the waveguide dimension variations beyond the limits of conventional microlithographic machines.

This research is sponsored by the BMDO and the U.S. Air Force Rome Lab..

6. REFERENCES

1. C. F. Janz, A. M. Gulisano, and R. G. Walker, "Improved fiber coupling to GaAs/AlGaAs rib waveguides using a regrowth-free mode drive-down technique," Electron. Lett., vol. 32, no. 11, pp. 1002-1004, 1996.
2. C. M. Weinert, "Design of fiber-matched uncladded rib waveguides on InP with polarization-independent mode matching loss of 1 dB," IEEE Photonics Technol. Lett., vol. 8, no. 8., pp. 1049-1051, 1996.
3. R. Zengerle, O. Leminger, W. Weiershausen, K. Faltin, and B. Hubner, "Laterally tapered InP-InGaAsP waveguides for low-loss chip-tp-fiber but coupling: a comparison of different configurations," IEEE Photonics Technol. Lett., vol. 7, no. 5., pp. 532-534, 1995.
4. M. Cheong, J. W. Seo, and Y. K. Jhee, "High alignment tolerance coupling scheme for multichannel laser diode/singlemode fiber modules using a tapered waveguide array," Electron. Lett., vol. 30, no. 18, pp. 1515-1517, 1994.
5. K. Mizuuchi, K. Yamamoto and T. Taniuchi, "High-efficiency coupling of laser diodes in tapered proton-exchanged waveguides," Electron. Lett., vol. 26, no. 24, pp. 1992-1994, 1992.

6. A. Fenner Milton and William K. Burns, "Mode coupling in optical waveguide horn," IEEE Journal of Quantum Electron., vol. QE-13, no. 10, pp. 828-835, 1977.
7. Ray. T. Chen, Suning Tang, T. Jannson and J. Jannson, "A 45-cm long compression-molded polymer-based optical bus," Appl. Phys. Lett., vol. 1032-1034, 1993.
8. Kohji Mimmi, Yoshio Yoshida, and Yukio Kurata, "Slant-propagation characteristics in tapered optical waveguides: analysis,", vol. 33, no. 34, pp. 8014-8021, 1994.
9. Z. N. Lu, Rajeev Bansal, and Peter K. Cheo, "Radiation losses of tapered dielectric waveguides: A finite difference analysis with ridge waveguide applications," J. of Lightwave Technol., vol. 12, no. 8, pp. 1373-1377,1994.
10. C. Vassallo, "Analysis of tapered mode transformers for semiconductor optical amplifiers," Optical and Quantum Electron., vol. 26, pp. S235-248, 1994.
11. A. Dendane and J. M. Arnold, "Beam radiation from tapered waveguides," IEEE Journal of Quantum Electron., vol. QE-22, no. 9, pp. 1551-1556, 1986.
12. C. H. Henry and Y. Shani, "Analysis of mode propagation in optical waveguide devices by Fourier expansion," IEEE J. Quantum Electron., vol. 27, pp. 523-530, 1991.
13. R. G. Hunsperger, A. Yariv and A. Lee, "Parallel end-butt coupling for optical integrated circuits," Appl. Opt., vol. 16, no. 4, pp. 1026-1032, 1987.
14. D. Marcuse, "Loss analysis of single-mode fiber splices," BSTJ, vol. 56, no. 5, pp. 703-719, 1977.
15. Suning Tang, Ray. T. Chen and Dave Gerold, "Channel cross-coupling in a polymer-based bus array," IEEE J. of Light. Technol., Vol. 13, No. 1, pp. 37-41, 1995.
16. F. P. Shovartsman, "Dry Photopolymer Embossing," Proc. SPIE, 1507, 383-391(1991)
17. Joel Frados, Plastic Engineering Handbook (Van Nostrand Reinhold Company).
18. C. A. Harper, ed., Electronic Packaging and Interconnection Handbook (McGraw-Hill, Inc., 1991).
19. C. A. Harper, Handbook of Plastics and Elastomers (McGraw-Hill Book Company, 1976).
20. R. Juran (ed.), Modern Plastics Encyclopedia, McGraw-Hill, New York, 1985.
21. Ray T. Chen, W. Phillips, D. Pelka and T. Jannson, "Gelatin waveguides in conjunction with integrated holographic optical elements in GaAs, $LiNbO_3$, glass and aluminum substrates for optical signal processing," Opt. Lett., vol. 14, pp. 892-895, 1989.
22. Ray T. Chen, "Graded index linear and curved polymer channel waveguides for massively parallel optical interconnects, "Appl. Phys. Lett. vol. 61, pp. 2278-2280, 1992.
23. R. Shih, Ray T. Chen, and Z. Z. Ho, "Traveling wave polymer waveguide modulator using coplanar electrode structure," SPIE, vol. 1774, pp. 11-18, 1992.
24. Ray T. Chen, L. Sadovnic, T. Jannson and J. Jannson, "Single-mode Polymer Waveguide Modulator," , Appl. Physics Lett., vol. 57, pp. 2071-2073, 1991.
25. Suning Tang and Ray. T Chen, "1-to-42 optoelectronic interconnect for clock signal distribution in wafer-scale VLSI multichip modules", Appl. Phy. Lett., Vol. 64, pp. 2931-2933, 1994.
26. Suning Tang, Rob Mayer, Maggie M. Li, Luke Graham, and Ray T. Chen, "A novel wavelength-division-demultiplexer with optical in-plane to surface-normal conversion," IEEE Photon. Technol. lett., Vol. 7, No. 8, pp. 908-910, 1995.
27. Ray T. Chen, Z. Z. Ho and D. Robinson, "Graded index polymer waveguide amplifier," Post Deadline Paper, Proc. SPIE, vol. 1774, pp. 39-44, 1992.